We are IntechOpen,
the world's leading publisher of
Open Access books
Built by scientists, for scientists

6,900
Open access books available

186,000
International authors and editors

200M
Downloads

154
Countries delivered to

Our authors are among the

TOP 1%
most cited scientists

12.2%
Contributors from top 500 universities

CLARIVATE ANALYTICS

BOOK CITATION INDEX

INDEXED

WEB OF SCIENCE™

Selection of our books indexed in the Book Citation Index
in Web of Science™ Core Collection (BKCI)

Interested in publishing with us?
Contact book.department@intechopen.com

Numbers displayed above are based on latest data collected.
For more information visit www.intechopen.com

Analytical and Numerical Solutions of Richards' Equation with Discussions on Relative Hydraulic Conductivity

Fred T. Tracy

U.S. Army Engineer Research and Development Center
USA

1. Introduction

Hydraulic conductivity is of central importance in modelling both saturated and unsaturated flow in porous media. This is because it is central to Darcy's Law governing flow velocity and Richards' equation that is often used as the governing partial differential equation (PDE) for unsaturated flow. When doing numerical modelling of groundwater flow, two dominant challenges regarding hydraulic conductivity are heterogeneous media and unsaturated flow.
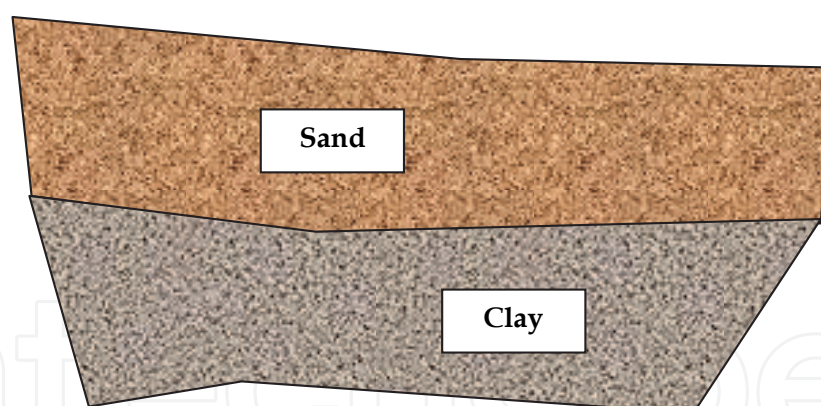

Fig. 1. Heterogeneous soil layers.

1.1 Heterogeneous media

Fig. 1 shows an example of soil layers full of heterogeneities that must be approximated in some way. Fig. 2 shows an idealization of a two-dimensional (2-D) cross section of a levee. Several layers representing different soil types are shown here. It is important to note that each layer is represented by a constant value of horizontal and vertical hydraulic conductivity rather than, for instance, a statistical variation. This is often done in numerical models and will be implemented in this work. The hydraulic conductivity values for sand and gravel are two to four times those of the silt and clay.
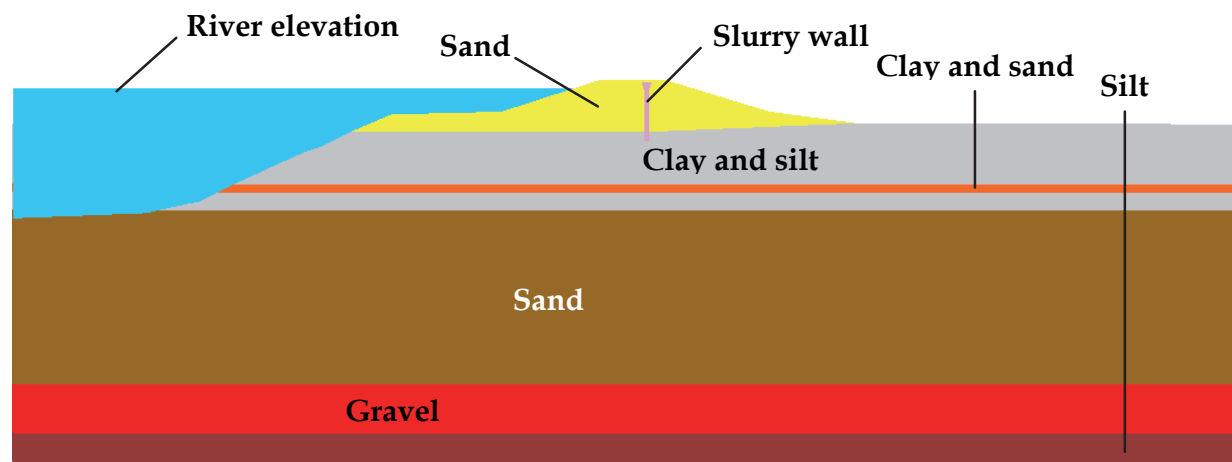
Fig. 2. Levee cross section with several soil types and a slurry wall.

An additional complexity is added in this problem by inserting the slurry wall. This type of wall is typically much less pervious than the surrounding soil, creating further stress on the computational model. This is because the numerical solution that is usually done requires a solution of a system of simultaneous, linear equations. The greater the span of orders of magnitude of hydraulic conductivity, the more challenging the solution of this system becomes.

1.2 Unsaturated flow

The last major concern and challenge discussed in this chapter regarding hydraulic conductivity with regard to computational and analytical solutions is unsaturated flow. Fig. 3 shows the location of the phreatic surface for steady-state conditions. The phreatic surface is where the ground goes from fully saturated when the soil voids are completely filled with water to partially saturated voids in the soil matrix. Above this phreatic surface, hydraulic conductivity is often modelled by
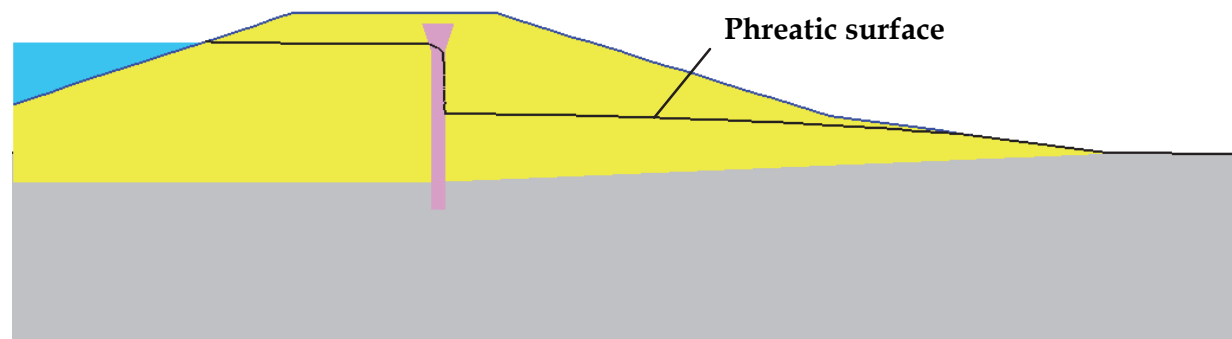
Fig. 3. Location of the phreatic surface at steady-state conditions.

$$k = k_r k_s \tag{1}$$

where

k = hydraulic conductivity of a given soil type

k_s = hydraulic conductivity for saturated soil

k_r ⠀⠀⠀= relative hydraulic conductivity for unsaturated soil

k_r is set to 1 in the saturated zone, but varies with the pressure head (h) in the unsaturated zone. There are many expressions for relative hydraulic conductivity in the literature and practice. Some of these will be discussed later in this chapter.

1.3 Obtaining computational results

A discretization of the flow region must be done to do the numerical analysis. Many techniques are available, but in this chapter, the finite element method (Cook, 1981) will be emphasized. Fig. 4 shows a zoom of the finite element mesh for the 2-D levee cross section given in Fig. 2 consisting of triangular elements. Define the total head as
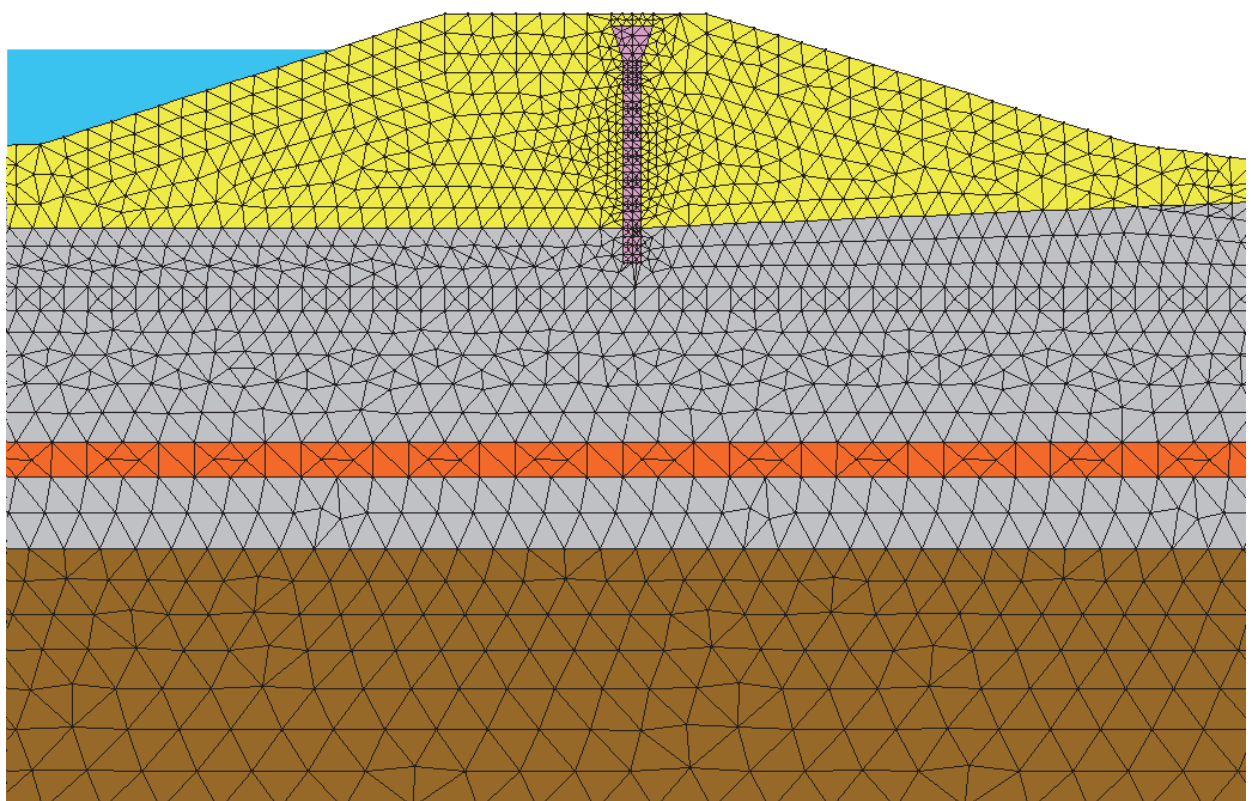

Fig. 4. Portion of the triangular mesh for the levee cross section.

$$\phi = h + z \qquad (2)$$

where

h ⠀⠀⠀= pressure head

ϕ ⠀⠀⠀= total head

z ⠀⠀⠀= z coordinate or elevation

Then equipotentials or total head contours can be used as a good way to visualize the data computed at each node of the mesh. Fig. 5 shows this type of plot for the levee example.
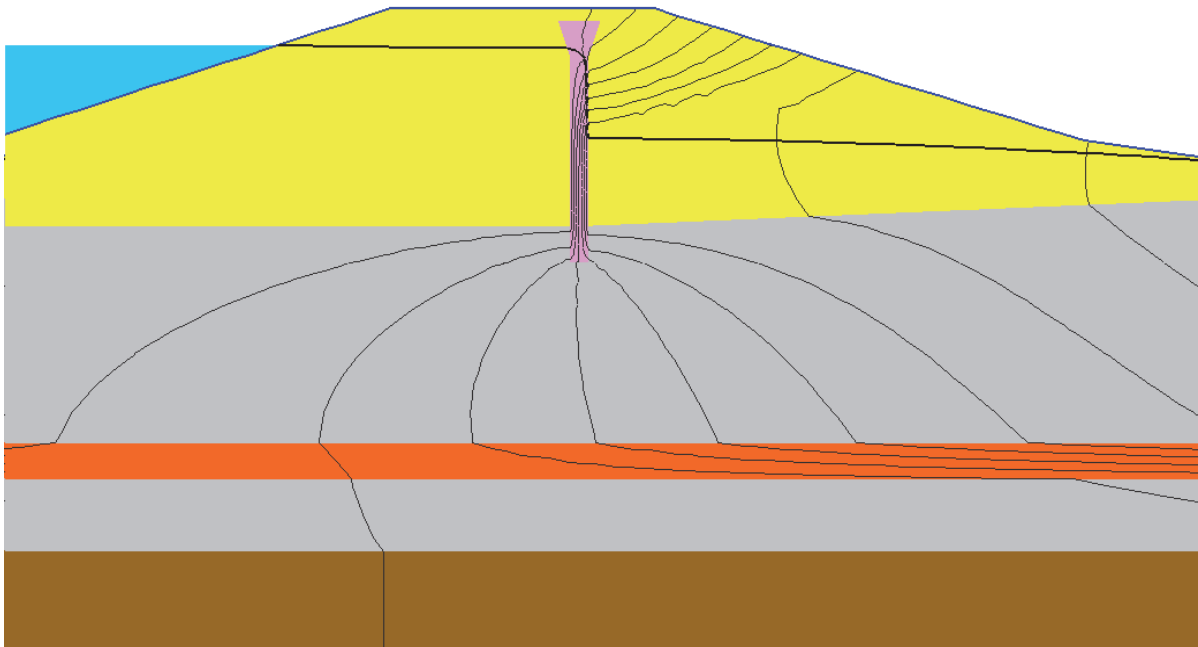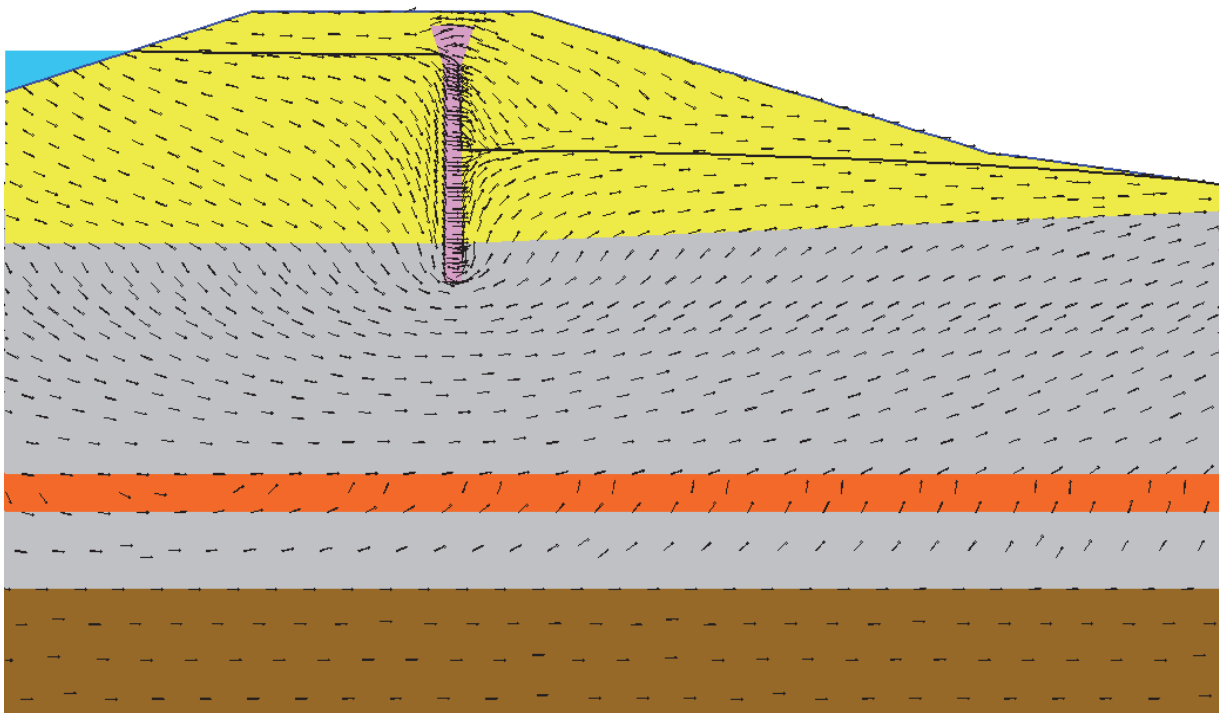
Fig. 5. Total head contours and phreatic surface.

Fig. 6. Velocity vectors and phreatic surface.

Finally, using Darcy's Law for a homogeneous medium,

$$\mathbf{v} = -k\nabla\phi \qquad (3)$$

where
$\mathbf{v}$ = flow velocity

A plot of velocity vectors for the levee cross section can be computed and plotted (see Fig. 6).

2. Relative hydraulic conductivity

One common way of representing relative hydraulic conductivity is using the van Genuchten expression (van Genuchten, 1980). First,

$$S_e = \left[1 + \zeta \left(-h \right)^n \right]^{-m}, \quad m = 1 - \frac{1}{n}, \quad h \leq 0$$
$$= 1, \quad h \geq 0$$
(4)

where

S_e = effective saturation

ζ = parameter based on soil type

n = parameter based on soil type

Then,

$$k_r = \sqrt{S_e} \left[1 - \left(1 - S_e^{1/m} \right)^m \right]^2, \quad h \leq 0$$
$$= 1, \quad h \geq 0$$
(5)

A simpler but less useful expression for relative hydraulic conductivity is the Gardner formulation (Gardner, 1958),

$$k_r = e^{\alpha h}$$
(6)

where

α = parameter based on soil type

Eq. 6 is shown here because this simpler equation is needed in the derivation of analytical solutions given later in this chapter. Regardless of the middle part of the curves, all relative hydraulic conductivity equations go from 1 at $h = 0$ to near 0 for negative values of h. In all these discussions, pressure head is greater than zero for saturated flow, equal to zero at the phreatic surface, and less than zero in the unsaturated zone.

3. Richards' equation

A common way of characterizing unsaturated flow is Richards' equation (Richards, 1931). A general version of this equation is

$$\nabla \cdot \left(\mathbf{K} \cdot \nabla \phi \right) = \frac{\partial \theta}{\partial t}$$
(7)

where

$\mathbf{K}$ = hydraulic conductivity tensor

θ = moisture content

t = time

For a homogeneous, isotrophic medium, $\mathbf{K}$ becomes k times the identity matrix, so after using Eqs. 1 and 2, Eq. 7 becomes,

$$\nabla \cdot \left(k_r \nabla h \right) + \frac{\partial k_r}{\partial z} = \frac{1}{k_s} \frac{\partial \theta}{\partial t} \tag{8}$$

Eq. 8 will be used for deriving the analytical solutions. The fact that k_r is a function of h creates significant difficulty both for solving this problem numerically and deriving analytical solutions since now Eq. 8 is often severely nonlinear.

4. Analytical solutions

Analytical solutions are an excellent tool for checking numerical programs for accuracy. In these derivations, hydraulic conductivity plays an important role. The challenge is finding a form of relative hydraulic conductivity such that the nonlinear Richards' equation can be converted from a nonlinear to a linear form. The derivations presented here are mirrored after those presented earlier (Tracy, 2006, 2007) because they lend themselves to one-dimensional (1-D), 2-D, and three-dimensional (3-D) solutions. First, 1-D and 2-D analytical solutions will be derived, and then numerical finite element solutions highlighting accuracy for different representations of relative hydraulic conductivity will be investigated.

4.1 1-D analytical solution of the Green-Ampt problem

Fig. 7 shows the 1-D problem that will be considered in detail. A column of soil of height, L, is initially dry until water begins to infiltrate the soil. A pool of water at the ground surface is then maintained holding the pressure head to zero. This is known as the 1-D Green-Ampt problem (Green & Ampt, 1911).
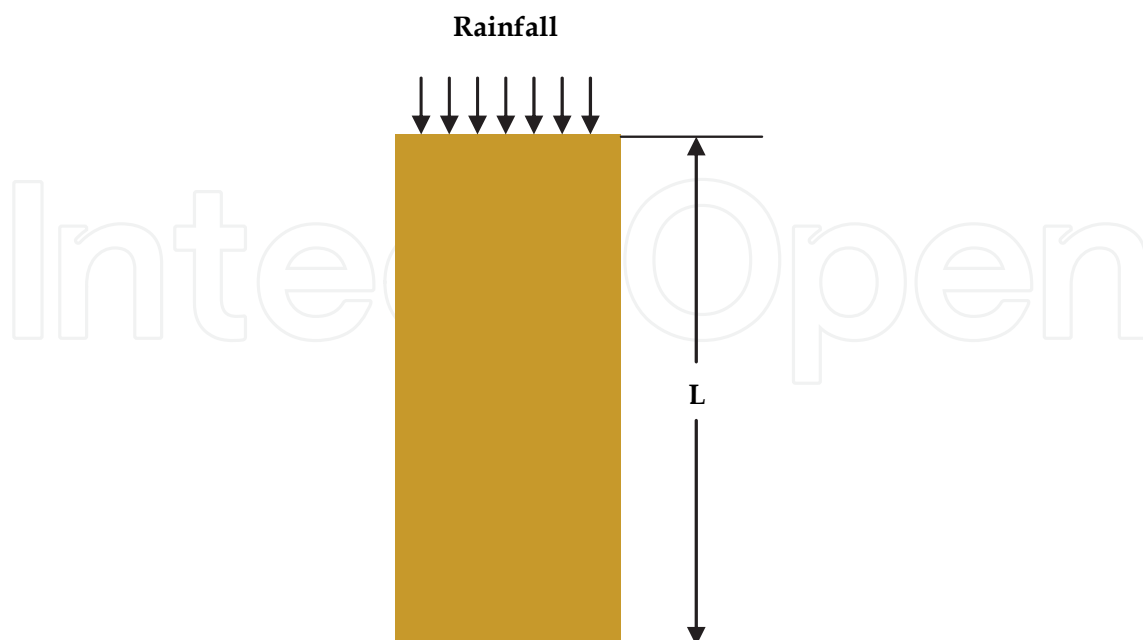

Fig. 7. A view of a 1-D column of soil that is initially dry until water is applied at the top of the ground surface from rainfall.

This problem is challenging numerically because the change in relative hydraulic conductivity is so dramatic, as it goes from small to one. There are several steps that are involved in the derivation for this problem, and they will now be summarized.

1. Provide a function of relative hydraulic conductivity and moisture content as a function of pressure head.
2. Establish initial and boundary conditions.
3. Perform a change of variables to linearize Richards' equation.
4. Solve this new PDE for the steady-state solution.
5. Obtain yet another PDE using a second change of variables.
6. Use separation of variables.
7. Use Fourier series to solve the current PDE.
8. Transform back to the original variables.

4.1.1 Relative hydraulic conductivity and moisture content

Gardner's equation (Eq. 6) is used for relative hydraulic conductivity, and moisture content is given by

$$\theta = \theta_d + (\theta_s - \theta_d) S_e \tag{9}$$

where

θ_d = moisture content when the soil is dry

θ_s = moisture content when the soil is saturated

Rather than use the van Genuchten expression for S_e, a simpler version is used (Warrick, 2003) as follows:

$$S_e = k_r \tag{10}$$

This equation is more limiting in actual practical application, but it allows easier derivation of the analytical solution. It is certainly good enough to test different computational strategies in computer programs.

4.1.2 Initial and boundary conditions

The initial conditions are that the soil is dry. Thus,

$$h(z,0) = h_d \tag{11}$$

where

h_d = the pressure head when the soil is dry

At $t > 0$, the boundary conditions at $z = 0$ and $z = L$ (top of the soil sample or at the ground surface) are

$$\begin{aligned} h(0,t) &= h_d \\ h(L,t) &= 0 \end{aligned} \tag{12}$$

4.1.3 Change of variables

The 1-D version of Eq. 8 is

$$\frac{\partial}{\partial z}\left(k_r\frac{\partial h}{\partial z}\right)+\frac{\partial k_r}{\partial z}=\frac{1}{k_s}\frac{\partial \theta}{\partial t} \tag{13}$$

Let the new variable, $\bar{h}$, be defined as

$$\bar{h}=e^{\alpha h}-\varepsilon,\quad \varepsilon=e^{\alpha h_d} \tag{14}$$

Then

$$\frac{\partial \bar{h}}{\partial z}=\alpha e^{\alpha h}\frac{\partial h}{\partial z} \tag{15}$$

and therefore,

$$k_r\frac{\partial h}{\partial z}=e^{\alpha h}\left(\frac{1}{\alpha}e^{-\alpha h}\frac{\partial \bar{h}}{\partial z}\right)=\frac{1}{\alpha}\frac{\partial \bar{h}}{\partial z} \tag{16}$$

In a similar manner,

$$\frac{\partial k_r}{\partial z}=\alpha e^{\alpha h}\frac{\partial h}{\partial z}=\frac{\partial \bar{h}}{\partial z} \tag{17}$$

and

$$\frac{\partial \theta}{\partial t}=(\theta_s-\theta_r)\frac{\partial S_e}{\partial t}=(\theta_s-\theta_r)\frac{\partial k_r}{\partial t}=(\theta_s-\theta_r)\frac{\partial \bar{h}}{\partial t} \tag{18}$$

Putting Eqs. 15-18 into Eq. 13 gives

$$\frac{\partial^2 \bar{h}}{\partial z^2}+\alpha\frac{\partial \bar{h}}{\partial z}=c\frac{\partial \bar{h}}{\partial t},\quad c=\frac{\alpha(\theta_s-\theta_d)}{k_s} \tag{19}$$

with initial conditions,

$$\bar{h}(z,0)=0 \tag{20}$$

and boundary conditions for $t>0$ from Eq. 12,

$$\begin{aligned}\bar{h}(0,t)&=0\\\bar{h}(L,t)&=1-\varepsilon\end{aligned} \tag{21}$$

4.1.4 Steady-state solution

The steady-state version of Eq. 19 will now be solved. It is important to note that this steady-state version now becomes an ordinary differential equation (ODE) as follows:

$$\frac{d^2\overline{h}_{ss}}{dz^2} + \alpha\frac{d\overline{h}_{ss}}{dz} = 0 \tag{22}$$

where $\overline{h}_{ss}$ is the steady-state solution. The general solution to this equation is

$$\overline{h}_{ss} = A_1 + A_2e^{-\alpha z} \tag{23}$$

where A_1 and A_2 are constants to be evaluated. When applying the boundary conditions of Eq. 21, the result is

$$\begin{aligned} 0 &= A_1 + A_2 \\ 1-\varepsilon &= A_1 + A_2e^{-\alpha L} \\ A_2 &= -A_1 \\ A_1 &= \frac{1-\varepsilon}{1-e^{-\alpha L}} \end{aligned} \tag{24}$$

The steady-state solution then becomes

$$\begin{aligned} \overline{h}_{ss}(z) &= (1-\varepsilon)\frac{1-e^{-\alpha z}}{1-e^{-\alpha L}} \\ &= (1-\varepsilon)\frac{e^{-\left(\frac{\alpha}{2}z\right)}\left(\dfrac{e^{\left(\frac{\alpha}{2}z\right)}-e^{-\left(\frac{\alpha}{2}z\right)}}{2}\right)}{e^{-\left(\frac{\alpha}{2}L\right)}\left(\dfrac{e^{\left(\frac{\alpha}{2}L\right)}-e^{-\left(\frac{\alpha}{2}L\right)}}{2}\right)} \\ &= (1-\varepsilon)e^{\frac{\alpha}{2}(L-z)}\frac{\sinh\left(\dfrac{\alpha}{2}z\right)}{\sinh\left(\dfrac{\alpha}{2}L\right)} \end{aligned} \tag{25}$$

4.1.5 Another transformation
Yet another transformation is now applied to Eq. 19. Define

$$\hat{h} = \overline{h} - \overline{h}_{ss} \tag{26}$$

Eq. 19 now becomes

$$\frac{\partial^2\left(\hat{h}+\overline{h}_{ss}\right)}{\partial z^2} + \alpha\frac{\partial\left(\hat{h}+\overline{h}_{ss}\right)}{\partial z} = c\frac{\partial\left(\hat{h}+\overline{h}_{ss}\right)}{\partial t} \tag{27}$$

Now since $\overline{h}_{ss}$ is the steady-state solution (Eq. 22), then

$$\frac{\partial^2 \hat{h}}{\partial z^2} + \alpha \frac{\partial \hat{h}}{\partial z} + \frac{\partial^2 \overline{h}_{ss}}{\partial z^2} + \alpha \frac{\partial \overline{h}_{ss}}{\partial z} = c \frac{\partial \hat{h}}{\partial t} + c \frac{\partial \overline{h}_{ss}}{\partial t}$$

$$\frac{\partial^2 \hat{h}}{\partial z^2} + \alpha \frac{\partial \hat{h}}{\partial z} = c \frac{\partial \hat{h}}{\partial t} \tag{28}$$

with initial and boundary conditions,

$$\hat{h}(z,0) = -\overline{h}_{ss}, \quad \hat{h}(0,t) = \hat{h}(L,t) = 0 \tag{29}$$

4.1.6 Separation of variables

Eq. 28 can be solved using separation of variables. $\hat{h}$ will be cast into the form,

$$\hat{h}(z,t) = Z(z)T(t) \tag{30}$$

where $Z(z)$ is a function only of z, and $T(t)$ is a function only of t. Substituting Eq. 30 into Eq. 28 and dividing by ZT gives

$$T\frac{\partial^2 Z}{\partial z^2} + \alpha T \frac{\partial Z}{\partial z} = cZ \frac{\partial T}{\partial t}$$

$$\frac{1}{Z}\left(\frac{\partial^2 Z}{\partial z^2} + \alpha \frac{\partial Z}{\partial z}\right) = \frac{c}{T} \frac{\partial T}{\partial t} \tag{31}$$

The only nontrivial solution occurs when the left- and right-hand sides of Eq. 31 are set to the same arbitrary constant, η. Thus,

$$\frac{1}{Z}\left(\frac{\partial^2 Z}{\partial z^2} + \alpha \frac{\partial Z}{\partial z}\right) = \eta = \frac{c}{T} \frac{\partial T}{\partial t}$$

$$\frac{\partial^2 Z}{\partial z^2} + \alpha \frac{\partial Z}{\partial z} - \eta Z = 0, \quad c \frac{\partial T}{\partial t} - \eta T = 0 \tag{32}$$

This leads to the characteristic equations,

$$m_1^2 + \alpha m_1 - \eta = 0, \quad cm_2 - \eta = 0 \tag{33}$$

with solutions,

$$m_{1a} = \frac{-\alpha + \sqrt{\alpha^2 + 4\eta}}{2}, \quad m_{1b} = \frac{-\alpha - \sqrt{\alpha^2 + 4\eta}}{2}, \quad m_2 = \frac{\eta}{c} \tag{34}$$

The general solution for $\hat{h}$ now becomes

$$Z = a_1 e^{m_{1a}z} + a_2 e^{m_{1b}z}, \quad T = e^{m_2 t}$$

$$\hat{h} = ZT = \left(a_1 e^{m_{1a}z} + a_2 e^{m_{2b}z}\right)e^{m_2 t} \tag{35}$$

where a_1 and a_2 are determined by initial and boundary conditions. For a physically realizable system, $\eta < 0$. To eliminate the radicals and to cast in a form that helps realize the general nature of the solution, the choice,

$$\eta = -\frac{\alpha^2}{4} - \lambda_k^2, \quad \lambda_k = \frac{\pi}{L}k, \quad k = 0, 1, 2, \dots \tag{36}$$

is made. This gives

$$\hat{h}_k = \left(a_{1k} e^{m_{1a}z} + a_{2k} e^{m_{1b}z} \right) e^{m_2 t}$$

$$= \left(a_{1k} e^{i\lambda_k z} + a_{2k} e^{-i\lambda_k z} \right) e^{-\frac{\alpha}{2}z - \mu_k t}, \quad \mu_k = \frac{1}{c}\left(\frac{\alpha^2}{4} + \lambda_k^2 \right), \quad i = \sqrt{-1} \tag{37}$$

It is best to rewrite Eq. 37 in terms of sine and cosine series and two other constants, A_k and B_k, to be evaluated. Thus, for all non-negative integers, k,

$$\hat{h} = \sum_{k=0}^{\infty} \left(A_k \sin \lambda_k z + B_0 + B_k \cos \lambda_k z \right) e^{-\frac{\alpha}{2}z - \mu_k t} \tag{38}$$

However, $\hat{h} = 0$ at $z = 0$, so $B_0 = B_k = 0$ and the final form is

$$\hat{h} = \sum_{k=1}^{\infty} A_k \sin \lambda_k z \, e^{-\frac{\alpha}{2}z - \mu_k t} \tag{39}$$

4.1.7 Fourier series solution

A_k in Eq. 39 can be evaluated by using Fourier series. Starting with

$$\hat{h}(z,0) = \sum_{k=1}^{\infty} A_k \sin \lambda_k z \, e^{-\frac{\alpha}{2}z} \tag{40}$$

the result from using Eqs. 25 and 29 is

$$A_k = \frac{2}{L} \int_0^L e^{\frac{\alpha}{2}z} \hat{h}(z,0) \, dz$$

$$= -\frac{2(1-\varepsilon)}{L \sinh\left(\frac{\alpha}{2}L\right)} e^{\frac{\alpha}{2}L} \int_0^L \sinh\left(\frac{\alpha}{2}z\right) \sin \lambda_k z \, dz \tag{41}$$

The last item in determining $\hat{h}$ is to evaluate the integral,

$$I = \int_0^L \sinh\left(\frac{\alpha}{2}z\right)\sin\lambda_k z\, dz$$

$$= \frac{2}{\alpha}\cosh\left(\frac{\alpha}{2}z\right)\sin\lambda_k z\Big]_0^L - \frac{2\lambda_k}{\alpha}\int_0^L \cosh\left(\frac{\alpha}{2}z\right)\cos\lambda_k z\, dz$$

$$= -\frac{2\lambda_k}{\alpha}\int_0^L \cosh\left(\frac{\alpha}{2}z\right)\cos\lambda_k z\, dz$$

$$= -\frac{4\lambda_k}{\alpha^2}\sinh\left(\frac{\alpha}{2}z\right)\cos\lambda_k z\Big]_0^L - \frac{4\lambda_k^2}{\alpha^2}\int_0^L \sinh\left(\frac{\alpha}{2}z\right)\sin\lambda_k z\, dz$$

$$= \frac{4\lambda_k}{\alpha^2}\sinh\left(\frac{\alpha}{2}L\right)(-1)^{k+1} - \frac{4\lambda_k^2}{\alpha^2}I \qquad (42)$$

$$\left(1 + \frac{4\lambda_k^2}{\alpha^2}\right)I = \frac{4\lambda_k}{\alpha^2}\sinh\left(\frac{\alpha}{2}L\right)(-1)^{k+1}$$

$$I = \frac{\lambda_k}{\left(\dfrac{\alpha^2}{4} + \lambda_k^2\right)}\sinh\left(\frac{\alpha}{2}L\right)(-1)^{k+1}$$

$$= \frac{\lambda_k}{c\mu_k}\sinh\left(\frac{\alpha}{2}L\right)(-1)^{k+1}$$

The solution for $\hat{h}$ then becomes

$$\hat{h} = \frac{2(1-\varepsilon)}{Lc}e^{\frac{\alpha}{2}(L-z)}\sum_{k=1}^{\infty}(-1)^k\frac{\lambda_k}{\mu_k}\sin\lambda_k z\, e^{-\mu_k t} \qquad (43)$$

4.1.8 Transform back

The last remaining task is to convert back to the original coordinates using Eqs. 14, 25, and 26. Therefore,

$$\bar{h} = \hat{h} + \bar{h}_{ss}$$

$$= (1-\varepsilon)e^{\frac{\alpha}{2}(L-z)}\left[\frac{\sinh\left(\dfrac{\alpha}{2}z\right)}{\sinh\left(\dfrac{\alpha}{2}L\right)} + \frac{2}{LC}\sum_{k=1}^{\infty}(-1)^k\frac{\lambda_k}{\mu_k}\sin\lambda_k z\, e^{-\mu_k t}\right] \qquad (44)$$

$$h = \frac{1}{\alpha}\ln(\bar{h} + \varepsilon) \qquad (45)$$
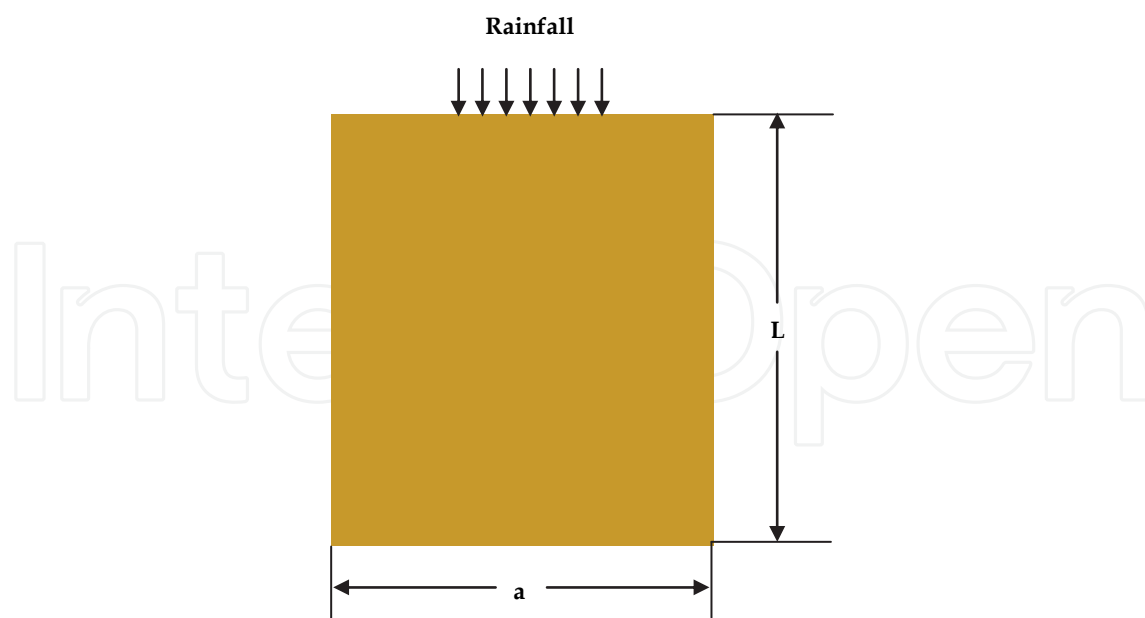
Rainfall

Fig. 8. A view of a 2-D cross section of soil that is initially dry until water is applied at the top

4.2 Analytical solution of a 2-D infiltration problem

The great thing about the above derivations is that they can be extended to two and three dimensions. Fig. 8 shows a 2-D cross section of a region of soil of dimensions, $a \times L$, where a 2-D Green-Ampt problem is presented. The soil is initially dry until water is supplied such that a specified pressure head is applied at the top with pressure head set to zero in the middle and tapering rapidly to h_d at $x = 0$ and $x = a$. Fig. 9 shows the function selected to achieve this for h_d = -20 m, and a = 50 m. $h = h_d$ is maintained along the bottom and sides of the soil sample as well. The initial and boundary conditions are therefore

$$h(x,z,0) = h_d \tag{46}$$

$$h(0,z,t) = h(a,z,t) = h(x,0,t) = h_d$$
$$h(x,L,t) = \frac{1}{\alpha} \ln \left\{ \varepsilon + (1-\varepsilon) \left[\frac{3}{4} \sin\left(\frac{\pi}{a} x\right) - \frac{1}{4} \sin\left(\frac{3\pi}{a} x\right) \right] \right\} \tag{47}$$

The equation for $\bar{h}$ is now

$$\frac{\partial^2 \bar{h}}{\partial x^2} + \frac{\partial^2 \bar{h}}{\partial z^2} + \alpha \frac{\partial \bar{h}}{\partial z} = c \frac{\partial \bar{h}}{\partial t} \tag{48}$$

with

$$\bar{h}(0,z,t) = \bar{h}(a,z,t) = \bar{h}(x,0,t) = 0$$
$$\bar{h}(x,L,t) = (1-\varepsilon) \left[\frac{3}{4} \sin\left(\frac{\pi}{a} x\right) - \frac{1}{4} \sin\left(\frac{3\pi}{a} x\right) \right] \tag{49}$$
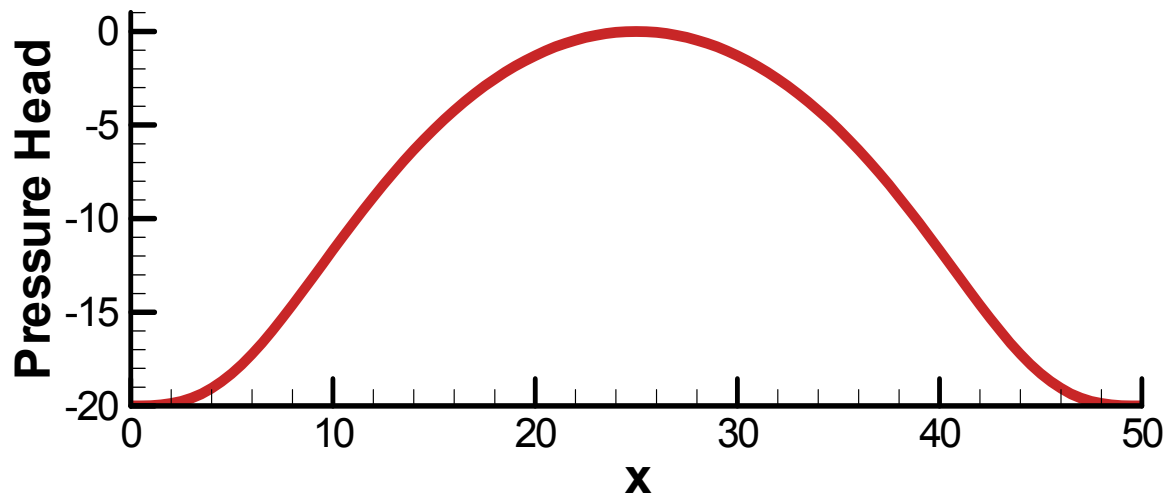
Fig. 9. Pressure head boundary condition applied at the top of the soil sample.

4.2.1 Steady-state solution for $\overline{h}$

The steady-state version of Eq. 48,

$$\frac{\partial^2 \overline{h}_{ss}}{\partial x^2} + \frac{\partial^2 \overline{h}_{ss}}{\partial z^2} + \alpha \frac{\partial \overline{h}_{ss}}{\partial z} = 0 \tag{50}$$

is now solved using separation of variables with $\overline{h}_{ss}$ taking the form,

$$\overline{h}_{ss} = \mathrm{X}(x)\mathrm{Z}(z) \tag{51}$$

This results in the equations,

$$\frac{1}{\mathrm{X}}\frac{\partial^2 \mathrm{X}}{\partial x^2} = -\lambda_i, \quad \frac{1}{\mathrm{Z}}\left(\frac{\partial^2 \mathrm{Z}}{\partial z^2} + \alpha \frac{\partial \mathrm{Z}}{\partial z}\right) = \lambda_i, \quad \lambda_i = \frac{\pi}{a}i, i = 0,1,2,\ldots$$

$$\frac{\partial^2 \mathrm{X}}{\partial x^2} + \lambda_i \mathrm{X} = 0, \quad \frac{\partial^2 \mathrm{Z}}{\partial z^2} + \alpha \frac{\partial \mathrm{Z}}{\partial z} - \lambda_i \mathrm{Z} = 0 \tag{52}$$

with solutions,

$$\mathrm{X}_i = a_i \sin \lambda_i x + b_i \cos \lambda_i x, \quad \mathrm{Z}_i = \left(c_i \sinh \beta_i z + d_i \cosh \beta_i z\right)e^{-\frac{\alpha}{2}z}, \quad \beta_i = \sqrt{\frac{\alpha^2}{4} + \lambda_i^2} \tag{53}$$

where a_i, b_i, c_i, and d_i are constants to be evaluated. Applying boundary conditions on the sides and bottom yields the final form of the steady-state solution as

$$\overline{h}_{ss} = e^{-\frac{\alpha}{2}z}\sum_{i=1}^{\infty} A_i \sin \lambda_i x \sinh \beta_i z \tag{54}$$

where A_i is a constant to be evaluated. Applying the top boundary condition gives

$$\overline{h}_{ss}(x,L) = e^{-\frac{\alpha}{2}L}\sum_{i=1}^{\infty}A_i\sin\lambda_i x\sinh\beta_i L$$

$$A_i = \frac{2(1-\varepsilon)e^{\frac{\alpha}{2}L}}{a\sinh\beta_i L}\int_0^a\left[\frac{3}{4}\sin\left(\frac{\pi}{a}x\right)-\frac{1}{4}\sin\left(\frac{3\pi}{a}x\right)\right]\sin\lambda_i x\,dx \qquad (55)$$

Only A_1 and A_3 are nonzero, so

$$A_1 = \frac{3(1-\varepsilon)e^{\frac{\alpha}{2}L}}{4\sinh\beta_1 L}, \quad A_3 = -\frac{(1-\varepsilon)e^{\frac{\alpha}{2}L}}{4\sinh\beta_3 L} \qquad (56)$$

The steady-state solution for $\overline{h}$ thus becomes

$$\overline{h}_{ss} = (1-\varepsilon)e^{\frac{\alpha}{2}(L-z)}\left[\frac{3}{4}\sin\left(\frac{\pi}{a}x\right)\frac{\sinh\beta_1 z}{\sinh\beta_1 L}-\frac{1}{4}\sin\left(\frac{3\pi}{a}x\right)\frac{\sinh\beta_3 z}{\sinh\beta_3 L}\right] \qquad (57)$$

4.2.2 Transient solution for $\hat{h}$

The equation for $\hat{h}$ is now

$$\frac{\partial^2\hat{h}}{\partial x^2}+\frac{\partial^2\hat{h}}{\partial z^2}+\alpha\frac{\partial\hat{h}}{\partial z}=c\frac{\partial\hat{h}}{\partial t} \qquad (58)$$

with initial and boundary conditions, as before,

$$\hat{h}(x,z,0) = -\overline{h}_{ss}, \quad \hat{h}(0,z,t) = \hat{h}(a,z,t) = \hat{h}(x,0,t) = \hat{h}(x,L,t) = 0 \qquad (59)$$

$\hat{h}$ now takes the form,

$$\hat{h} = X(x)Z(z)T(t) \qquad (60)$$

This yields

$$\frac{1}{X}\frac{\partial^2 X}{\partial x^2}+\frac{1}{Z}\left(\frac{\partial^2 Z}{\partial z^2}+\alpha\frac{\partial Z}{\partial z}\right)=\frac{c}{T}\frac{\partial T}{\partial t} \qquad (61)$$

and

$$\frac{1}{X}\frac{\partial^2 X}{\partial x^2}=-\lambda_i^2, \quad \frac{1}{Z}\left(\frac{\partial^2 Z}{\partial z^2}+\alpha\frac{\partial Z}{\partial z}\right)=-\lambda_k^2-\frac{\alpha^2}{4}, \quad \lambda_k=\frac{\pi}{L}k,$$

$$\frac{c}{T}\frac{\partial T}{\partial t}=-\left(\lambda_i^2+\lambda_k^2+\frac{\alpha^2}{4}\right), \quad i=1,2,3,\dots, \quad k=1,2,3,\dots \qquad (62)$$

The general solutions are

$$X_i = a_i \sin \lambda_i x + b_i \cos \lambda_i x, \quad Z = \left(c_k \sin \lambda_k z + d_k \cos \lambda_k z \right) e^{-\frac{\alpha}{2} z}$$

$$T = f_{ik} e^{-\gamma_{ik} t}, \quad \gamma_{ik} = \frac{1}{c} \left(\lambda_i^2 + \lambda_k^2 + \frac{\alpha^2}{4} \right) = \frac{1}{c} \left(\beta_i^2 + \lambda_k^2 \right) \tag{63}$$

with the final form of $\hat{h}$ being

$$\hat{h} = e^{-\frac{\alpha}{2} z} \sum_{k=1}^{\infty} \sum_{i=1}^{\infty} A_{ik} \sin \lambda_i x \sin \lambda_k z e^{-\gamma_{ik} t} \tag{64}$$

Here, a_i, b_i, c_k, d_k, f_{ik}, and A_{ik} are constants to be evaluated. Evaluating the above equation at $t = 0$ using the double Fourier sine series gives

$$A_{ik} = -\frac{4}{aL} \int_0^L \int_0^a \bar{h}_{ss} e^{\frac{\alpha}{2} z} \sin \lambda_i x \sin \lambda_k z \, dx \, dz \tag{65}$$

with the two nonzero terms with respect to i being

$$
\begin{aligned}
A_{1k} &= -\left(\frac{2}{L} \right) \frac{3}{4} (1 - \varepsilon) e^{\frac{\alpha}{2} L} \int_0^L \sin \lambda_k z \frac{\sinh \beta_1 z}{\sinh \beta_1 L} dz \\
&= \left(\frac{2}{Lc} \right) \frac{3}{4} (1 - \varepsilon) e^{\frac{\alpha}{2} L} \left(\frac{\lambda_k}{\gamma_{1k}} \right) (-1)^k \\
A_{3k} &= \left(\frac{2}{L} \right) \frac{1}{4} (1 - \varepsilon) e^{\frac{\alpha}{2} L} \int_0^L \sin \lambda_k z \frac{\sinh \beta_3 z}{\sinh \beta_3 L} dz \\
&= -\left(\frac{2}{Lc} \right) \frac{1}{4} (1 - \varepsilon) e^{\frac{\alpha}{2} L} \left(\frac{\lambda_k}{\gamma_{3k}} \right) (-1)^k
\end{aligned}
\tag{66}
$$

The solution for $\hat{h}$ now becomes

$$\hat{h} = \frac{2}{Lc} (1 - \varepsilon) e^{\frac{\alpha}{2}(L-z)} \left\{ \begin{array}{l} \dfrac{3}{4} \sin\left(\dfrac{\pi}{a} x \right) \displaystyle\sum_{k=1}^{\infty} \left(\dfrac{\lambda_k}{\gamma_{1k}} \right) (-1)^k \sin \lambda_k z - \\[2mm] \dfrac{1}{4} \sin\left(\dfrac{3\pi}{a} x \right) \displaystyle\sum_{k=1}^{\infty} \left(\dfrac{\lambda_k}{\gamma_{3k}} \right) (-1)^k \sin \lambda_k z \end{array} \right\} \tag{67}$$

As done before, transforming back to the original coordinates gives

$$\bar{h} = \frac{2}{Lc} (1 - \varepsilon) e^{\frac{\alpha}{2}(L-z)} \left\{ \begin{array}{l} \dfrac{3}{4} \sin\left(\dfrac{\pi}{a} x \right) \left[\dfrac{\sinh \beta_1 z}{\sinh \beta_1 L} + \dfrac{2}{Lc} \displaystyle\sum_{k=1}^{\infty} \left(\dfrac{\lambda_k}{\gamma_{1k}} \right) (-1)^k \sin \lambda_k z \right] - \\[3mm] \dfrac{1}{4} \sin\left(\dfrac{3\pi}{a} x \right) \left[\dfrac{\sinh \beta_3 z}{\sinh \beta_3 L} + \dfrac{2}{Lc} \displaystyle\sum_{k=1}^{\infty} \left(\dfrac{\lambda_k}{\gamma_{3k}} \right) (-1)^k \sin \lambda_k z \right] \end{array} \right\} \tag{68}$$

Also, as before, transforming back to the original h,

$$h = \frac{1}{\alpha} \ln \left(\bar{h} + \varepsilon \right) \qquad (69)$$

A 3-D solution is done in a similar manner.

5. Numerical models

Hydraulic conductivity has an important role in numerical models. Many soil layers can be modelled by specifying hydraulic conductivity for the different layers. Because Richards' equation is nonlinear, the manner in which numerical models compute relative hydraulic conductivity is also important for both accuracy of the solution and the ability of the numerical algorithms to converge. When doing a 3-D Green-Ampt problem containing thousands of 3-D finite elements on a parallel high performance computing platform, the solution would not converge because of how relative hydraulic conductivity was computed inside each finite element. When the pressure head was averaged from the four nodes of each tetrahedral element and then used to compute a constant value for the relative hydraulic conductivity inside the element, the solution diverged. However, if relative hydraulic conductivity was considered to vary linearly inside each element, the solution converged quite well. Testing these different algorithms is greatly enhanced by the analytical solutions presented above. Some tests using the analytical solutions will now be illustrated.

5.1 1-D solution of the Green-Ampt problem
The 1-D version of Eq. 7 for a homogeneous, isotropic soil is

$$k_s \frac{\partial}{\partial z} \left(k_r \frac{\partial \phi}{\partial z} \right) = \frac{\partial \theta}{\partial t} \qquad (70)$$

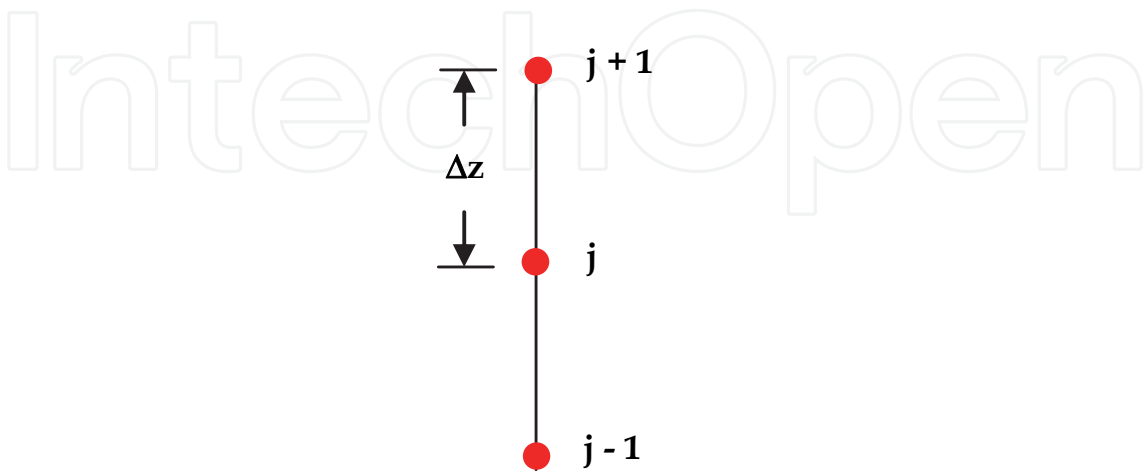A finite element/finite difference/finite volume discretization of this equation (see Fig. 10) is

Fig. 10. Discretization of the 1-D soil sample showing two finite elements.

$$k_{r+}\left(\phi_j^{n+1} - \phi_{j+1}^{n+1}\right) + k_{r-}\left(\phi_j^{n+1} - \phi_{j-1}^{n+1}\right) + \frac{\Delta z^2}{k_s \Delta t}\left(\frac{d\theta}{dh}\right)_j^{n+1}\left(\phi_j^{n+1} - \phi_j^n\right) = 0 \tag{71}$$

where

j	= node number
k_{r-}	= the relative hydraulic conductivity for the element between nodes j and $j-1$
k_{r+}	= the relative hydraulic conductivity for the element between nodes j and $j+1$
Δt	= time-step size
n	= time-step number

The two ways of computing relative hydraulic conductivity inside each element will now be discussed.

5.1.1 Constant relative hydraulic conductivity inside each element

This way of computing relative hydraulic conductivity is to first compute the average pressure head (h_{av}) at the center of the element. For k_{r+}, this becomes

$$h_{av} = \frac{1}{2}\left(h_j + h_{j+1}\right) \tag{72}$$

Then compute relative hydraulic conductivity by

$$k_{r+} = e^{\alpha h_{av}} \tag{73}$$

k_{r-} is computed in the same way.

5.1.2 Linearly varying relative hydraulic conductivity inside each element

This way of computing relative hydraulic conductivity is the equivalent of first computing the relative hydraulic conductivity at the node points. For nodes j and $j+1$, designate relative hydraulic conductivity by

$$k_{r,j} = e^{\alpha h_j}, \quad k_{r,j+1} = e^{\alpha h_{j+1}} \tag{74}$$

Averaging these values for the final result gives

$$k_{r+} = \frac{1}{2}\left(k_{r,j} + k_{r,j+1}\right) \tag{75}$$

k_{r-} is computed in the same way.

5.1.3 1-D numerical test results

The above equation was solved using L = 50 m; k_s = 0.1 m/day; h_d = -20 m; θ_d = 0.15; θ_s = 0.45; Δz = 0.25 m; α = 0.1 m-1, 0.2 m-1, and 0.3 m-1; and Δt = 0.01 day for 100 time-steps with the two versions of computing relative hydraulic conductivity. The model used was a simple FORTRAN program written by the author. The largest in absolute value (worst) error in pressure head for each method is given in Table 1. It is important to note that the

respective signs of these errors have been retained. From these results, it is seen that the
linearly varying version gave the best results.

α (1/m)	0.1	0.2	0.3
Constant k_r (m/day)	-0.12	-0.28	-0.43
Linear k_r (m/day)	-0.09	-0.12	0.17

Table 1. Worst error in pressure head for different values of α for constant and linearly
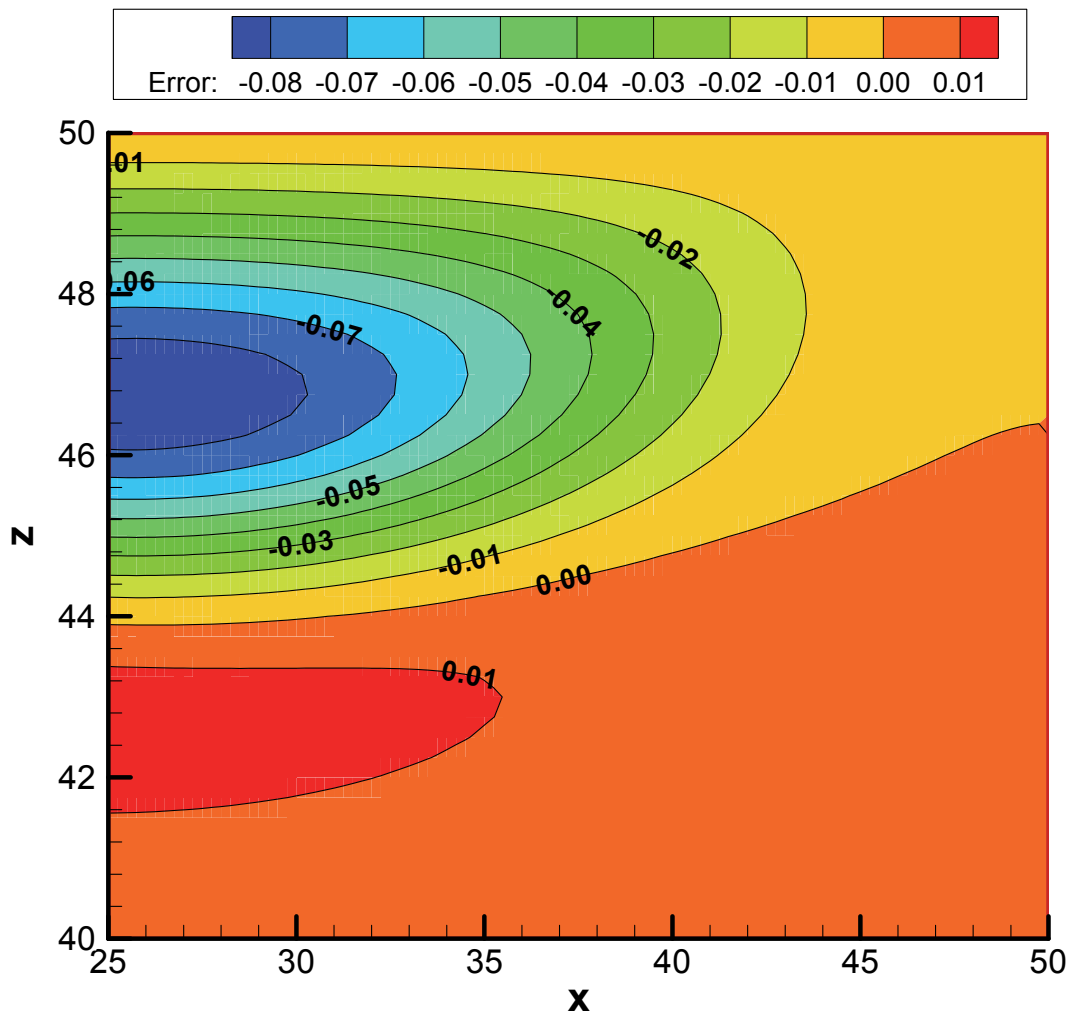varying k_r.

Fig. 11. Error plot for pressure head (h) for the upper, right-hand corner of the
computational region.

5.2 2-D solution of the Green-Ampt problem

The 2-D version of Eq. 7 was solved for the problem given in Section 4.2 with the values of
the parameters being the same as for the 1-D problem presented above but with the addition
of a = 50 m. The model used for this computation was a transient version of Seep2D (Tracy,
1983, & Seep2D, 2011). A steady-state version of Seep2D is currently incorporated into the

Groundwater Modeling System (GMS) (Jones, 1999, & GMS, 2011). The transient version is not yet available.

Fig. 11 gives a color contour plot of the error for the linearly varying relative hydraulic conductivity option for α = 0.1 m^{-1} for the upper, right-hand region of 10 m × 25 m. Clearly, the results match well with the analytical solution.

6. Summary

This chapter has shown that hydraulic conductivity plays an important role in both deriving analytical solutions and doing numerical computations. Analytical solutions for both the 1-D and 2-D Green-Ampt problem were derived and computed numerically with the results compared. The derivations are presented in such detail that others can do additional solutions as well. Varying relative hydraulic conductivity linearly within each finite element not only makes the nonlinear convergence algorithm more robust, but it also produces more accurate answers than when it is considered constant inside each finite element.

7. Acknowledgment

8. References

Cook, R. (1981). *Concepts and Applications of Finite Element Analysis* (2nd Edition), John Wiley & Sons, New York.

Gardner, W. (1958). Some steady-state solutions of the unsaturated moisture flow equation with application to evaporation from a water table. *Soil Science*, Vol. 85, pp. 228–232.

GMS. (2011). http://chl.erdc.usace.army.mil/gms.

Green, W., & Ampt, G. (1911). Studies on soil physics, part I, the flow of air and water through soils. *Journal of Agricultural Science*, Vol. 4, pp. 1-24.

Jones, N. (1999). Seep2D Primer. Groundwater Modeling System, Environmental Modeling Research Laboratory, Brigham Young University, Provo, Utah.

Richards, R. (1931). Capillary conduction of liquid through porous media. *Physics*, Vol. 1, pp. 318-333.

Seep2D. (2011). Wikipedia. http://en.wikipedia.org/wiki/SEEP2D.

Tracy, F. (1983). User's Guide for a Plane and Axisymmetric Finite Element Program for Steady-State Seepage Problems. Instruction Report No. IR K-83-4, Vicksburg, MS, U.S. Army Engineer Waterways Experiment Station.

Tracy, F. (2006). Clean two- and three-dimensional analytical solutions of Richards' equation for testing numerical solvers. *Water Resources Research*, Vol. 42, W08503.

Tracy, F. (2007). Three-dimensional analytical solutions of Richards' equation for a box-shaped soil sample with piecewise-constant head boundary conditions on the top. *Journal of Hydrology*, Vol. 336, pp. 391-400.

van Genuchten, M. (1980). A closed-form equation for producing the hydraulic conductivity of unsaturated soils. *Soil Science American Journal*, Vol. 44, pp. 892-898.

Warrick, A. (2003). *Soil Water Dynamics*, Oxford University Press, New York.
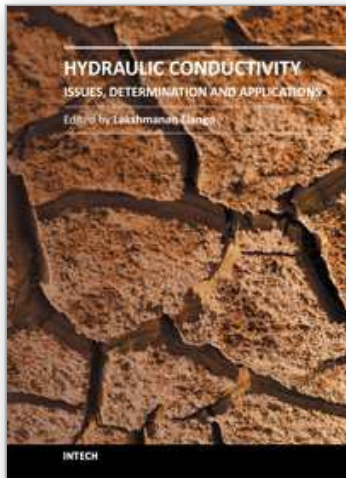
Hydraulic Conductivity - Issues, Determination and Applications

Edited by Prof. Lakshmanan Elango

There are several books on broad aspects of hydrogeology, groundwater hydrology and geohydrology, which do not discuss in detail on the intrigues of hydraulic conductivity elaborately. However, this book on Hydraulic Conductivity presents comprehensive reviews of new measurements and numerical techniques for estimating hydraulic conductivity. This is achieved by the chapters written by various experts in this field of research into a number of clustered themes covering different aspects of hydraulic conductivity. The sections in the book are: Hydraulic conductivity and its importance, Hydraulic conductivity and plant systems, Determination by mathematical and laboratory methods, Determination by field techniques and Modelling and hydraulic conductivity. Each of these sections of the book includes chapters highlighting the salient aspects and most of these chapters explain the facts with the help of some case studies. Thus this book has a good mix of chapters dealing with various and vital aspects of hydraulic conductivity from various authors of different countries.

How to reference

In order to correctly reference this scholarly work, feel free to copy and paste the following:

Fred T. Tracy (2011). Analytical and Numerical Solutions of Richards' Equation with Discussions on Relative Hydraulic Conductivity, Hydraulic Conductivity - Issues, Determination and Applications, Prof. Lakshmanan Elango (Ed.), ISBN: 978-953-307-288-3, InTech, Available from: http://www.intechopen.com/books/hydraulic-conductivity-issues-determination-and-applications/analytical-and-numerical-solutions-of-richards-equation-with-discussions-on-relative-hydraulic-condu